International Journal of Advances in Scientific Research and Engineering (ijasre)

E-ISSN : 2454-8006

DOI: 10.31695/IJASRE.2023.9.11.6

Volume 9, Issue 11
November - 2023

Mapping and Spatiotemporal Dynamics of Land-use and Land-cover Change Based on the USGS and NASA Platforms from MCD12Q1 Landsat Imagery: A Case Study of Kinshasa, DR Congo

Innocent MUFUNGIZI MIHIGO [1,2,3,4&5*], Trésor HUBERT KAWAYA [1,2], Roda BONGELI MBOPANGA [1,2], Jean KABULO BANZA [1,2], Ridi DIAKONDUA VUILAWO [1,2] & Ruben LOOLA LOKETO [1,2]

[1]Mention Earth Sciences, Faculty of Sciences and Technologies

University of Kinshasa, B.P. 190 Kinshasa XI, DR Congo

[2] LeGeolog Research Team, Kinshasa DR Congo

[3]Pedo-Geochemistry laboratory, Faculty of Sciences and Technologies, University of Kinshasa, DR Congo

[4]Medical Research Circle (MedRec), Goma, DR Congo

[5]The Marine Biological Association (MBA), Plymouth, United Kingdom

ABSTRACT

Kinshasa is a city with very significant urban growth. It is observed that this urban growth is concentrated in a weak area, which requires control and direction of urban expansion. To do this, it is important to understand the dynamics of cover change and land use over time. To do this, we downloaded Landsat images from the MODIS Land Cover Type Product (MCD12Q1) from 2001 to 2022, with a classification of these images based on remote sensing indices that we processed using geographic information system tools. We extracted the following classes: Evergreen Broadleaf Forests, Deciduous Broadleaf Forests, Mixed Forests, Closed Shrublands, Woody Savannas, Savannas, Grasslands, Permanent Wetlands, Croplands, Urban and Built-up Lands, Cropland/Natural Vegetation Mosaics, Barren and Water Bodies. We calculated the percentage of coverage of the classes taking into account intervals of 3 years (7 intervals in total) by studying the relationship between the evolution curves of these classes, but also, we established the relationship existing between the dynamics of these classes over time using the chord diagram. It has been observed that certain classes vary depending on others over time.

Keywords: Chord diagram, Land cover, Land use, MCD12Q1, Model builder.

1. INTRODUCTION

The survival of humanity depends on the natural resources available. It is necessary to improve the management of these resources and strengthen the knowledge on the interactions between humans and the earth through the resources available to them. To understand these interactions, the study of variations of land use/cover therefore becomes a very important source of information because it highlights anthropogenic activities and spatiotemporal change in the environment [1,2].

The city of Kinshasa is experiencing very significant urban growth, but urbanization is concentrated in a small area. This situation results from multiple causes which have limited the physical accessibility of the population to land resources: the very strong growth of the population, the saturation of road infrastructure, urban poverty and the low motorization with which it is associated [3].

Urban expansion would have occurred at a rate of 7.1 km²/year over these 27 years. In 1967, the census counted 901,520 people in Kinshasa and mentioned an average annual growth rate of 8% [4].

This rapid population growth results in increased demand for social and infrastructure services, education, health and other basic services that are essential to making the city habitable, which poses a challenge questions and concerns. The city of Kinshasa has been officially considered a megacity since 2013, because of the population which was 10 million [5,6]. Unfortunately, the growth observed is often very unorganized and has a direct link with the creation of avenues and informal neighborhoods [7]. These cases are observed in Kinshasa but they are observable in other cities of the Democratic Republic of Congo [8,9,10]. These problems affect the expanding peripheries through socio-economic and environmental impacts due to the absence of infrastructure and community services, long journeys to city centers, erosion, flooding, etc. [11,12,13,14].

Land cover is defined by the Food and Agriculture Organization (FAO) as the (bio)-physical coverage of the surface of the emerged land taking into account the type of use or non-use of these lands by humans [15]. Land cover includes all physical materials visible on the Earth's surface. The latter can be natural or resulting from anthropogenic activities and take up in their entirety the surfaces occupied by water, trees, grass, paving, bare soil, the surface occupied by buildings, etc. [16].
Several indices are used, including Normalized difference vegetation index (NDVI) [17,18], Ratio vegetation index (RVI) [19], Enhanced vegetation index (EVI) [20,21], Difference vegetation index (DVI) [22,23], Normalized difference water index (NDWI) [24,25], Normalized difference building vegetation index (NDBI) [25], Regulated soil vegetation index (SAVI) [26], Urban building index (IBI-A, IBI-B, IBI) [27,28].

The MODIS Land Cover Type Product (MCD12Q1) provides a suite of science datasets (SDSs) that map global land cover at annual time step for six different land cover legends. The maps were created from classifications of Spectro temporal features derived from data from the Moderate Resolution Imaging Spectroradiometer (MODIS) [29]. With the aim of studying the dynamics of land cover in Kinshasa (quantitatively and qualitatively evaluating the evolution of land use classes over time) to understand the evolution of the coverage surface of the different classes and their interactions under different methods in the period from 2001 to 2022, we used data acquired by remote sensing that we processed and analyzed using geographic information system techniques and statistical analysis tools in order to be able to give a conclusion of the work. This study contributes to a knowledge base that can help research environmental balance, ecosystem preservation and sustainable development planning by studying interactions between classes.

2. METHODS

To achieve the objectives set, we downloaded on-site data from United State Geological Survey (USGS) Earth Explorer and National Aeronotics Space Agency (NASA) which presented data from 2001 to 2022 for the area including Kinshasa which is the study area shown in figure 1.

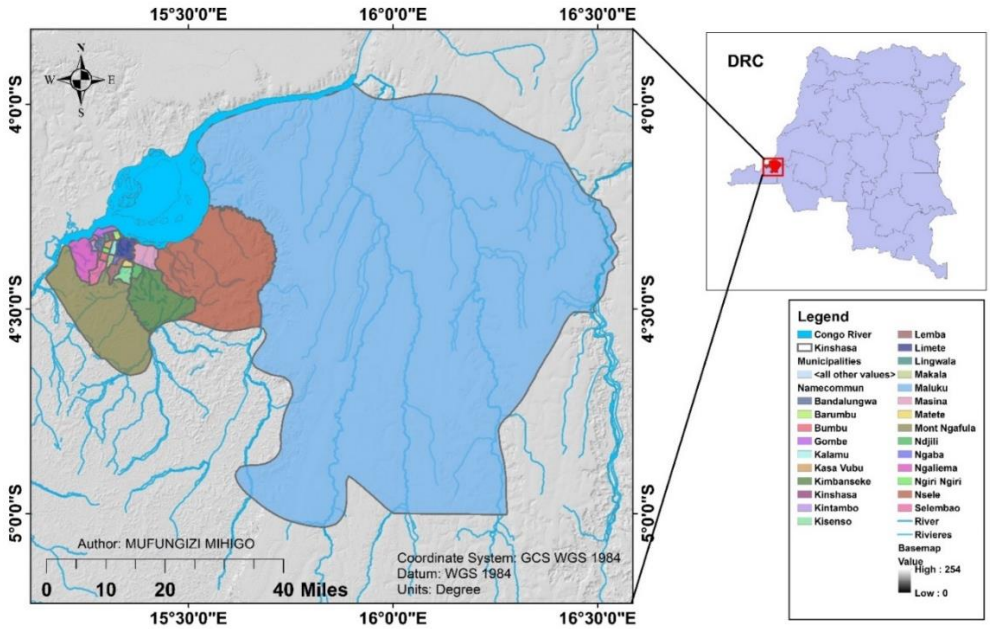

Fig. 1. Location map of the study area

DOI: 10.31695/IJASRE.2023.9.11.6

We chosed a 3-year interval by first analyzing data from the earliest year available, then from 2001 to 2004; from 2004 to 2007; from 2007 to 2010; from 2010 to 2013; from 2013 to 2016; from 2016 to 2019; and finally 2019 to 2022 which is the most recent year available. The following table shows information about the downloaded data.

Table 1. Presentation of unprocessed data

Entity ID	Year	Visualization	Entity ID	Year	Visualization
MCD12Q1.A2001001.h19v09.061	-2001	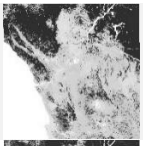	**MCD12Q1.A2012001.h19v09.061**	2012	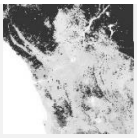
MCD12Q1.A2002001.h19v09.061	2002	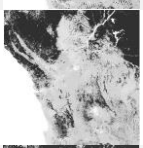	**MCD12Q1.A2013001.h19v09.061**	2013	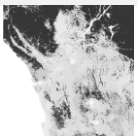
MCD12Q1.A2003001.h19v09.061.2022151163011	2003	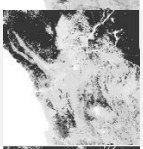	**MCD12Q1.A2014001.h19v09.061**	2014	
MCD12Q1.A2004001.h19v09.061	2004	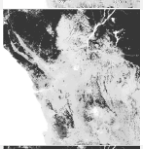	**MCD12Q1.A2015001.h19v09.061**	2015	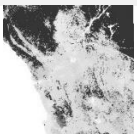
MCD12Q1.A2005001.h19v09.061	2005	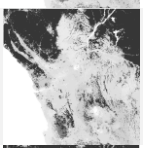	**MCD12Q1.A2016001.h19v09.061**	2016	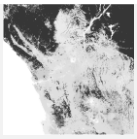
MCD12Q1.A2006001.h19v09.061	2006		**MCD12Q1.A2017001.h19v09.061**	2017	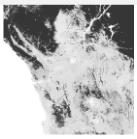
MCD12Q1.A2007001.h19v09.061	2007	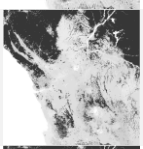	**MCD12Q1.A2018001.h19v09.061**	2018	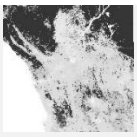
MCD12Q1.A2008001.h19v09.061	2008	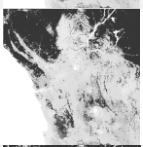	**MCD12Q1.A2019001.h19v09.061**	2019	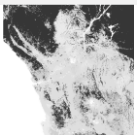
MCD12Q1.A2009001.h19v09.061.	2009	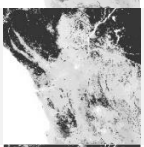	**MCD12Q1.A2020001.h19v09.061**	2020	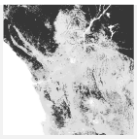
MCD12Q1.A2010001.h19v09.061	2010	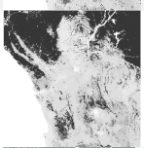	**MCD12Q1.A2021001.h19v09.061**	2021	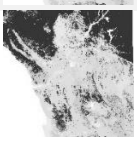
MCD12Q1.A2011001.h19v09.061	2011	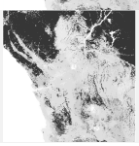	**MCD12Q1.A2022001.h19v09.061**	2022	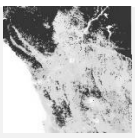

The data thus obtained was processed using geographic information system (GIS) tools, particularly ArcGIS software. For statistical analyses, we used Excel and OriginPro software.

DOI: 10.31695/IJASRE.2023.9.11.6

3. RESULTS AND DISCUSSIONS

The classes studied are: Evergreen Broadleaf Forests, Deciduous Broadleaf Forests, Mixed Forests, Closed Shrublands, Woody Savannas, Savannas, Grasslands, Permanent Wetlands, Croplands, Urban and Built-up Lands, Cropland/Natural Vegetation Mosaics, Barren and Water Bodies.
The description of the classes was made following the description guide presented in table 2.

Table 2. MCD12Q1 International Geosphere-Biosphere Programme (IGBP) legend and class descriptions [29].

Name	Value	Description
Evergreen Needleleaf Forests	1	Dominated by evergreen conifer trees (canopy >2m). Tree cover >60%.
Evergreen Broadleaf Forests	2	Dominated by evergreen broadleaf and palmate trees (canopy >2m). Tree cover >60%.
Deciduous Needleleaf Forests	3	Dominated by deciduous needleleaf (larch) trees (canopy >2m). Tree cover >60%.
Deciduous Broadleaf Forests	4	Dominated by deciduous broadleaf trees (canopy >2m). Tree cover >60%.
Mixed Forests	5	Dominated by neither deciduous nor evergreen (40-60% of each) tree type (canopy >2m). Tree cover >60%.
Closed Shrublands	6	Dominated by woody perennials (1-2m height) >60% cover.
Open Shrublands	7	Dominated by woody perennials (1-2m height) 10-60% cover.
Woody Savannas	8	Tree cover 30-60% (canopy >2m).
Savannas	9	Tree cover 10-30% (canopy >2m).
Grasslands	10	Dominated by herbaceous annuals (<2m).
Permanent Wetlands	11	Permanently inundated lands with 30-60% water cover and >10% vegetated cover.
Croplands	12	At least 60% of area is cultivated cropland.
Urban and Built-up Lands	13	At least 30% impervious surface area including building materials, asphalt, and vehicles.
Cropland/Natural Vegetation Mosaics	14	Mosaics of small-scale cultivation 40-60% with natural tree, shrub, or herbaceous vegetation.
Permanent Snow and Ice	15	At least 60% of area is covered by snow and ice for at least 10 months of the year.
Barren	16	At least 60% of area is non-vegetated barren (sand, rock, soil) areas with less than 10% vegetation.
Water Bodies	17	At least 60% of area is covered by permanent water bodies.
Unclassified	255	Has not received a map label because of missing inputs.

DOI: 10.31695/IJASRE.2023.9.11.6

For data processing with geographic information system tools, we used the model builder shown here in figure 2. First we use the Extract by mask tool in Spatial Analyst Tools by putting MCD12Q1 as Input raster and the Kinshasa shapefile as Input raster or feature mask data. As input we have a multiband raster file with its attribute values.
The mask is specified in the environment parameter when running the Extract by Mask tool, the output raster has cell values only for the area at the intersection of the environment mask and the data in the input mask. The default output format is a geodatabase raster.
Secondly, we use the raster obtained from the first step (Output raster) as Input raster in the raster to polygon conversion tool using the values.
The input raster can be any cell size and must be a valid integer raster dataset. We have chosen the attribute field of the input raster dataset which becomes an attribute in the output feature class.
The polygon obtained will finally be used in the dissolve tool using the gridcode to give the area occupied by the land cover classes.

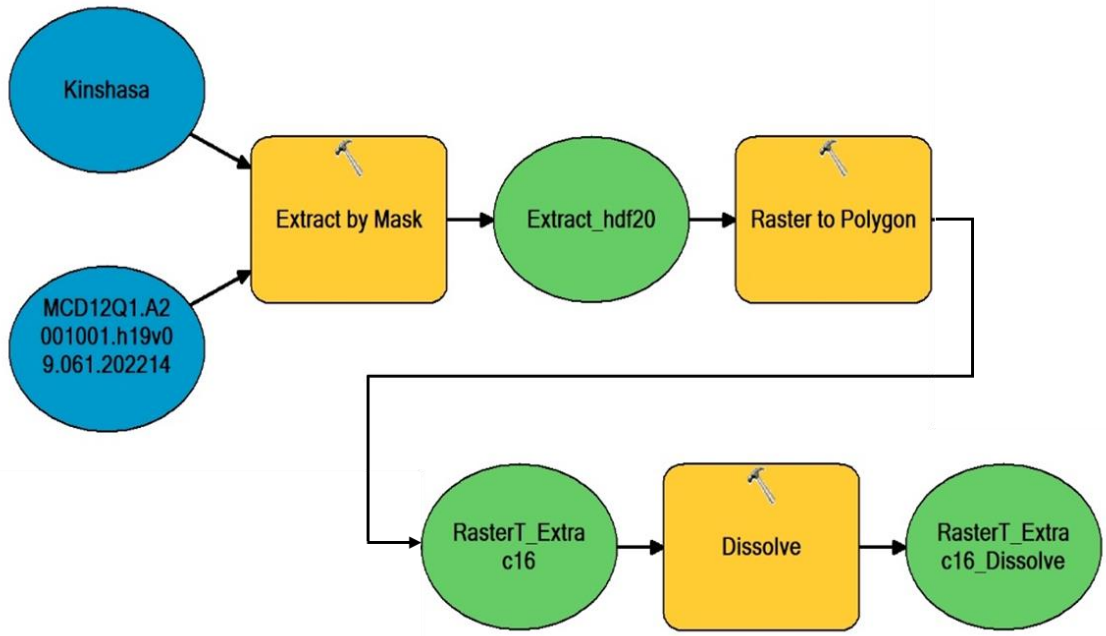

Fig. 2. Model builder of data processing

Data processing was done in ArcGIS using the tools available in ArcToolBox by appying the model builder shown in the figure above. After extraction and processing, we have had the results in figure 3.

DOI: 10.31695/IJASRE.2023.9.11.6

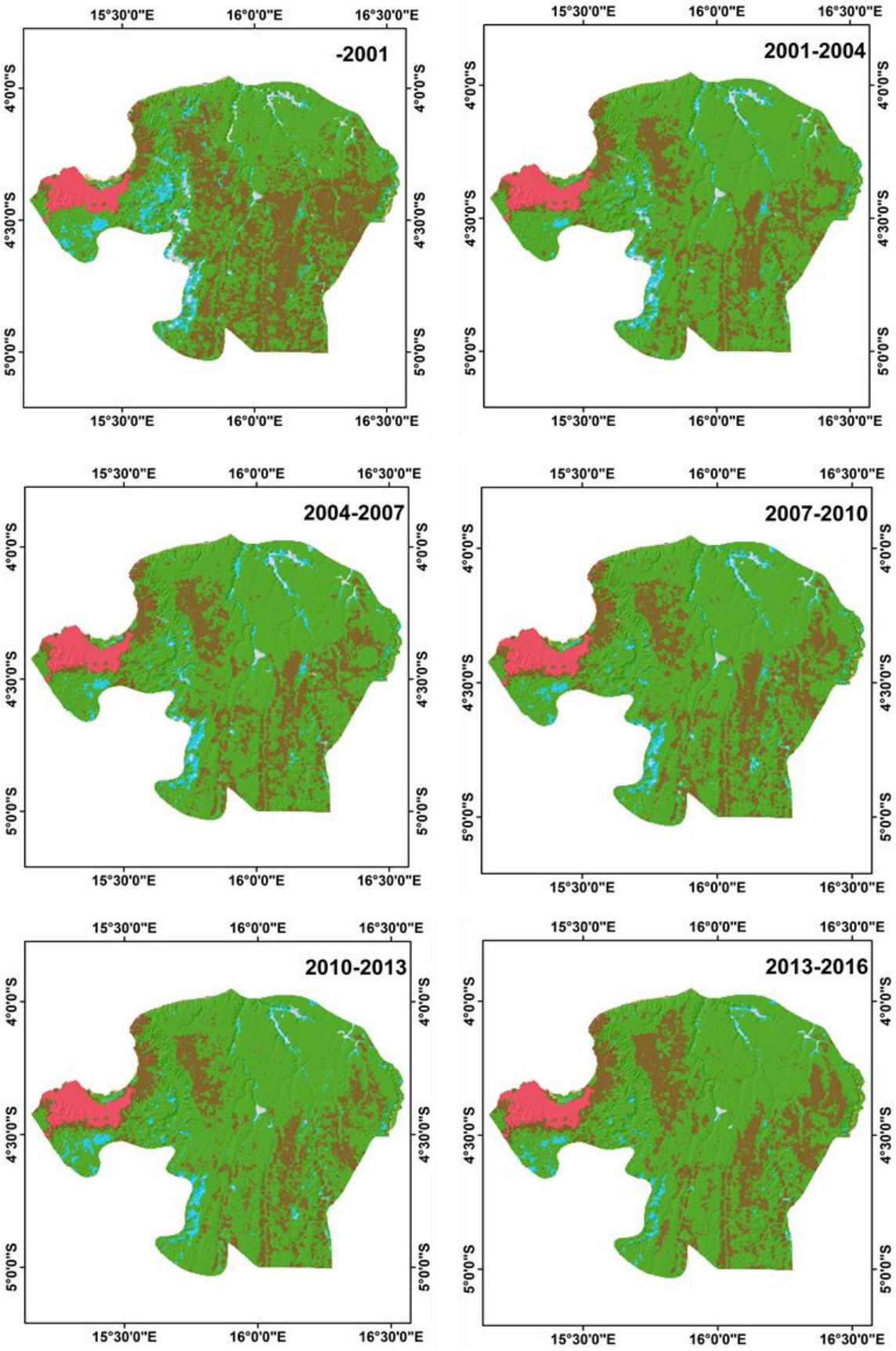

Fig. 3. Land cover and land use of Kinshasa (2001-2016)

DOI: 10.31695/IJASRE.2023.9.11.6

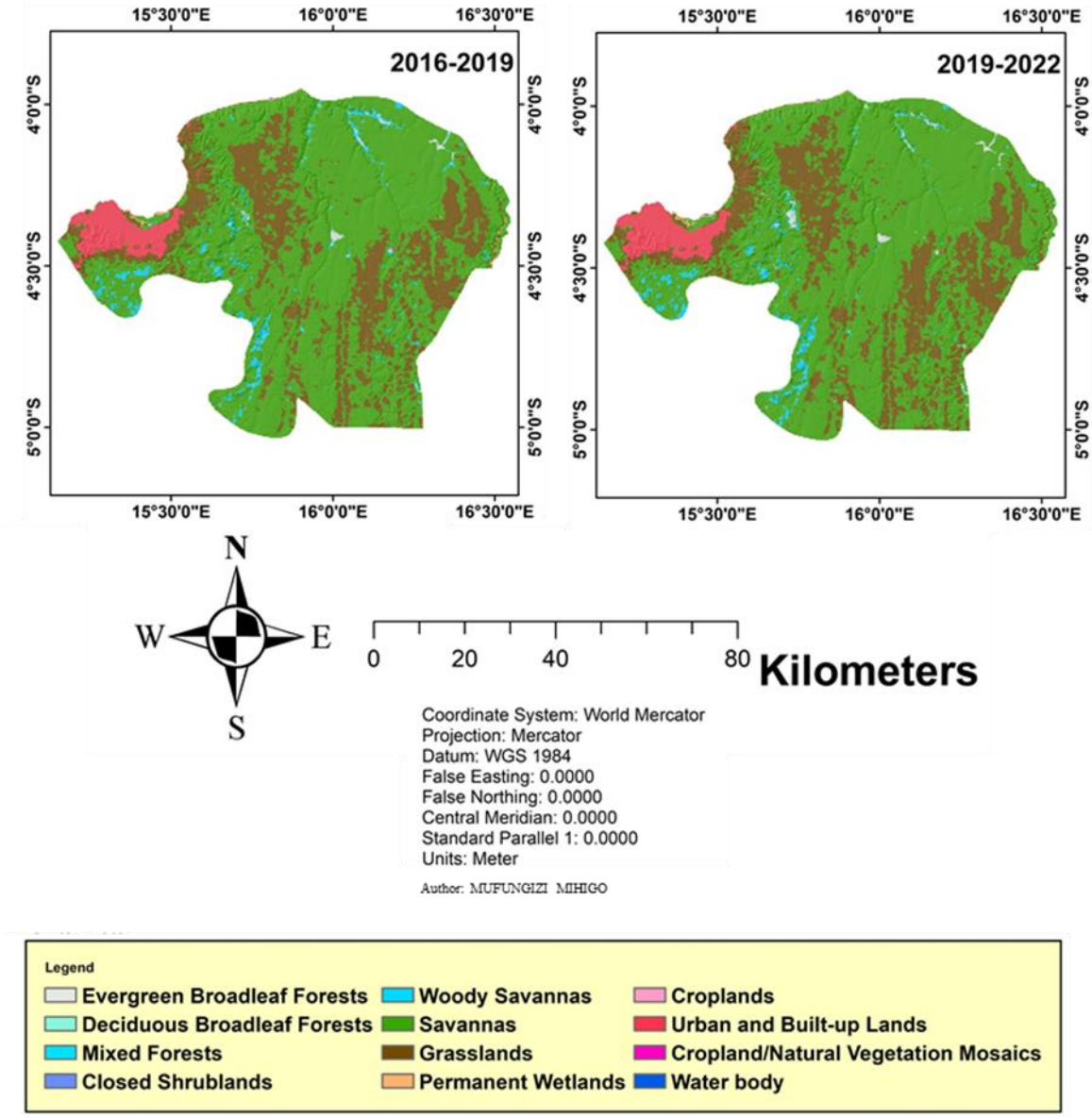

Fig. 3. *Continued* (2016-2022)

To study the dynamics of land use evolution, it is important to take time and space into account. To do this, we converted the Rasters into polygons based on the values describing the classes. We then used the dissolve tool in ArcGIS based on the grid code to determine the coverage area of each class.

The results of this processing phase are presented as percentages by year interval following classes in table 3.

DOI: 10.31695/IJASRE.2023.9.11.6

Table 3. Percentage of land cover and land use for each class in the study period

CLASS	GRIDCODE	PERCENT						
		2001	2004	2007	2010	2013	2016	2019	2022
EVERGREEN BROADLEAF FORESTS	2	1.4835	1.22035	0.743076	0.597613	0.464224	0.339395	0.309965	0.480767
DECIDUOUS BROADLEAF FORESTS	4	0.0073	0	0.00136	0	0	0	0	0
MIXED FORESTS	5	0.0133	0	0.002632	0.03732	0.036278	0	0	0
CLOSED SHRUBLANDS	6	0.0053	0.04587	0.013443	0.021154	0.003346	0.005959	0.001272	0
WOODY SAVANNAS	8	4.8055	3.22498	3.245325	3.445348	3.364137	2.386075	2.398213	2.091478
SAVANNAS	9	56.2332	74.140926	71.760721	69.68632	72.393328	68.756595	68.768172	67.933466
GRASSLANDS	10	33.0503	17.192015	20.159899	22.013064	19.629244	24.391233	24.344705	25.242677
PERMANENT WETLANDS	11	0.5298	0.314571	0.207616	0.31316	0.203675	0.212031	0.241288	0.259943
CROPLANDS	12	0.0206	0	0	0.00136	0	0	0	0
URBAN AND BUILT-UP LANDS	13	3.8292	3.853343	3.85997	3.878703	3.899809	3.900768	3.930426	3.977765
CROPLAND/NATURAL VEGETATION MOSAICS	14	0.0073	0	0	0	0	0	0	0
BARREN	16	0.0000	0.0000	0.0000	0.0000	0.0000	0.001986	0.001986	0.001986
WATER BODIES	17	0.0147	0.007945	0.005959	0.005959	0.005959	0.005959	0.003972	0.011917

To understand the evolution of each class, we processed the data in table 3 to produce the following figures:

DOI: 10.31695/IJASRE.2023.9.11.6

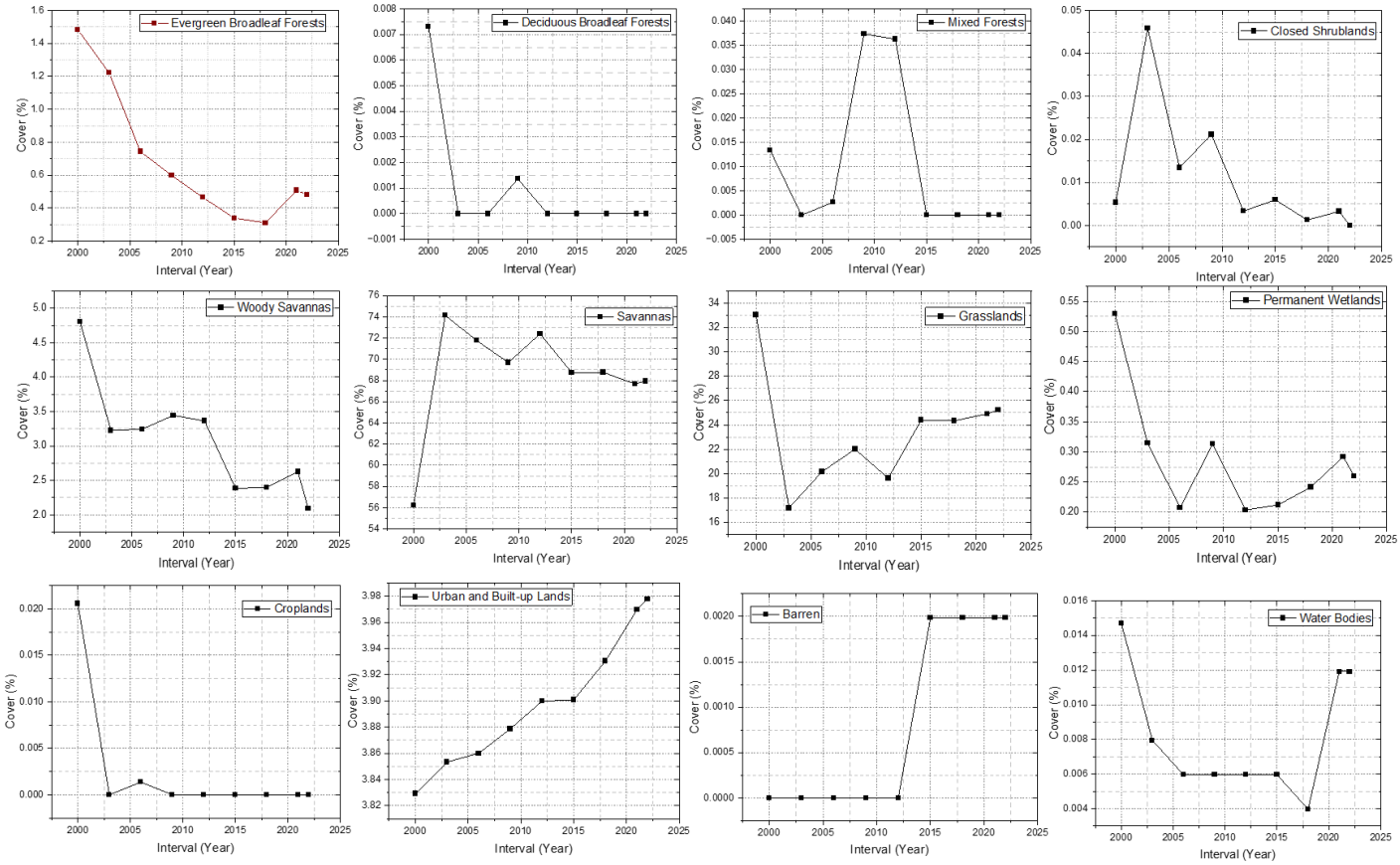

Fig. 4a. Dynamics of classes taken one by one

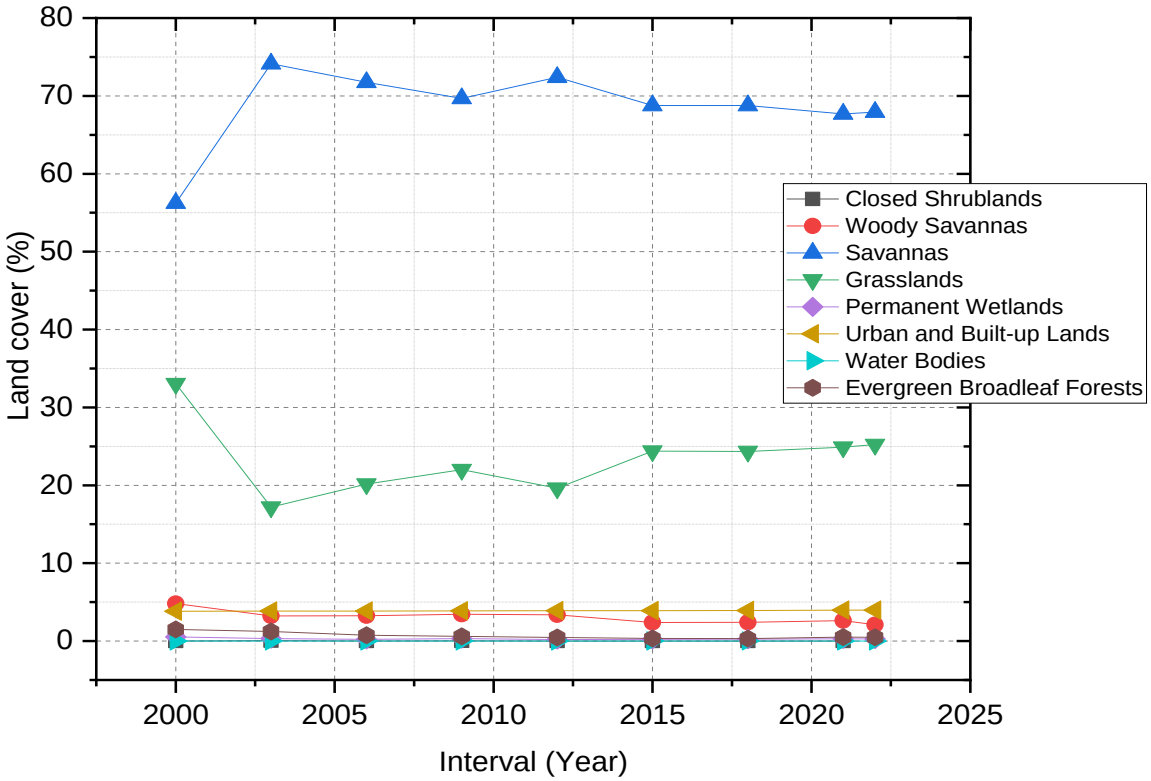

Fig. 4b. Class Dynamics Comparison Diagram

The interpretation of figures 4a and 4b shows the following:

- Evergreen Broadleaf Forests: shows a loss of regular cover percentage until 2019, then a slight increase;
- Deciduous Broadleaf Forests: suffered a total loss of percentage cover from 2001 to 2007 where it recovered slightly for a total loss until 2022;
- Mixed Forests: shows strong growth in coverage area in the period from 2010 to 2013 and finally falls completely until 2022;

DOI: 10.31695/IJASRE.2023.9.11.6

- Closed Shrublands: reached a peak in 2004, then a regression until 2022 with a trend of recovery in 2010;
- Woody Savannas: We notice a decrease in the coverage area during the study period;
- Savannas: this class is the one with the greatest percentage of coverage, we note that it presents a peak in 2004 and the dynamic is regular over time compared to other classes;
- Grasslands: This class is second only to Savannas in terms of coverage percentage. It suffered a decline until 2013, then a slight and irregular rise until 2022;
- Permanent Wetlands: This class has three trends. It decreases from 2001 to 2007, then shows growth in 2010, then decreases in 2013 and finally shows growth until 2022;
- Croplands: presents a total fall;
- Urban and Built-up Lands: this class shows regular growth over time;
- Barren: This class appears in 2016 and presents regular coverage until 2022;
- Water Bodies: this class decreases until 2007, it remains regular until 2016 to decrease again in 2019 and finally rise while remaining regular in 2022.

To understand the relationships between classes, we used chord diagram (figure 5). A chord diagram is a graphical method of displaying inter-relationships between data radially around a circle. It represents flows or connections between several entities (called nodes) with the relationships between the nodes typically drawn as arcs connecting the data. Here the size of the arc is proportional to the importance of the flow. Chord diagrams are used to visualize data ranging from business use cases to complex scientific data [30].

This figure shows the relationships between classes. It is observable that certain classes are closely related such as the Woody Savannas and the Savannas. When the first decreases, the second increases and this can be explained by deforestation. It is the same for the Grasslans and Permanent Wetlands, their curves have the same appearance. The regular evolution of Urban and Built-up Lands directly impacts the other classes although on the 21-year scale, it seems small compared to the area studied.

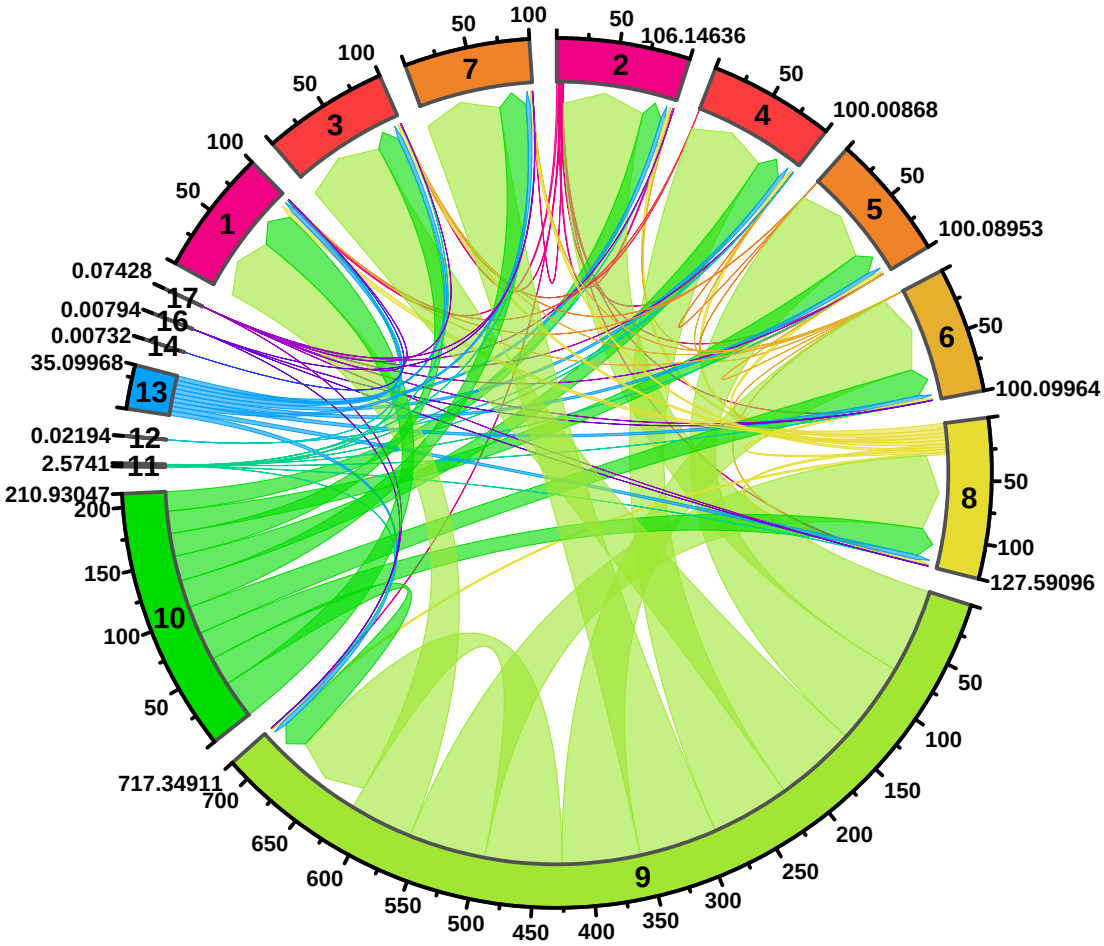

Fig. 5. Chord diagram of land cover and land use (%) form 2001 to 2022

DOI: 10.31695/IJASRE.2023.9.11.6

4. CONCLUSION

This study is based on Landsat images from the MODIS Land Cover Type Product (MCD12Q1) with a classification of these images based on remote sensing indices. We found the following land use and cover classes: Evergreen Broadleaf Forests, Deciduous Broadleaf Forests, Mixed Forests, Closed Shrublands, Woody Savannas, Savannas, Grasslands, Permanent Wetlands, Croplands, Urban and Built-up Lands, Cropland /Natural Vegetation Mosaics, Barren and Water Bodies. After calculating the coverage area of these classes, we studied the variation of the percentage of their coverage over time and the relationships existing between these classes. It was noted that the variation in the percentage coverage of certain classes depends on other classes. This is the case of Woody Savannas and the Savannas; Grasslands and Permanent Wetlands. The Urban and Built-up Lands class presents a regular and continuous evolution over time but remains concentrated in one area. Future investigations should focus on data spanning many years with higher resolution. The processing must focus on high-precision algorithms to achieve impeccable results with a minimum of error on cover and land use classes.

SUPPLEMENTARY INFORMATION

Acknowledgments

Not applicable.

Authors' contributions

Conceptualization: IM; Design: IM; Investigation: IM; Project administration: IM; Resources: All authors; Software: IM; Supervision: IM & JK; Validation: All authors; Visualization: All authors; Roles/Writing - original draft; IM; Writing - review & editing: All authors.

Availability of data and materials

The data used for this study will be made available upon reasonable request.

Funding

The authors did not receive any funding for this study.

Declarations

Compliance with Ethical Standards: This article does not contain any studies involving human or animal subjects.

Competing interests: The authors declare that there are no conflicts of interest.

REFERENCES

[1] G. Sun, Z. Pan, A. Zhang, X. Jia, J. Ren, H. Fu, K. Yan (2023). Large kernel spectral and spatial attention networks for hyperspectral image classification, IEEE Trans. Geosci. Rem. Sens. 61 5519915 (Early Access). **DOI**: 10.1109/TGRS.2023.3292065

[2] C. Chen, J. Liang, F. Xie, Z. Hu, W. Sun, G. Yang, J. Yu, J. Chen, L.H. Wang, L.Y. Wang, H.X. Chen, X.Y. He, Z. Zhang (2022). Temporal and spatial variation of coastline using remote sensing images for Zhoushan archipelago, China, Int. J. Appl. Earth Obs. Geoinf. 107, 102711. https://doi.org/10.1016/j.jag.2022.102711

[3] Jean-Pierre M. N., Kouagou R. S., Philippes M. F., Jean-Pierre M. M., Jan B. and Jean-Marie H. (2019). La croissance de l'urbanisation morphologique à Kinshasa entre 1979 et 2015 : Analyse Densimétrique Et De La Fragmentation Du Bâti. BSGLg, 73, 2019, 85-103. Available at: https://popups.uliege.be/0770-7576/index.php?id=5937&file=1

[4] Eléonore W**.** and Virginie D. (2002). Extension urbaine et densité de la population à Kinshasa : contribution de la télédétection satellitaire. https://doi.org/10.4000/belgeo.15451

[5] INS (2015). Annuaire statistique 2014. Kinshasa: RDC, Ministère du Plan et Révolution de la Modernité, Institut Nationale de la Statistique.

[6] SOSAK (2014). Schéma d'orientation stratégique de l'agglomération kinoise et plan particulier d'aménagement de la zone nord de la ville. Kinshasa : RDC, Gouvernement provinciale de Kinshasa

[7] Watson, V. (2009). The planet city sweeps the poor away,'*: Urban planing and the 21st century urbanisation. **Progress in Planning, 72**, 151-193.

DOI: 10.31695/IJASRE.2023.9.11.6

[8] Useni, S., Cabala, K., Halleux, J.-M., Bogaert, J. & Munyemba, K. (2018). Caractérisation de la croissance spatiale urbaine de la ville de Lubumbashi (Haut-Katanga, R.D. Congo) entre 1989 et 2014. **Tropicultura, 36**(1), 99-108.

[9] De Saint Moulin, L. (2010). **Ville et organisation de l'espace en République Démocratique du Congo.** Paris: L'Harmattan.

[10] Flouriot, J. (2008). Congo RDC : Population et Aménagement d'un Immense Pays. **Population et Avenir, 2** (687), 4-8.

[11] Lelo Nzuzi, F. (2018). **Les bidonvilles de Kinshasa.** Paris: L'Harmattan

[12] Angel, S., Cievco, D. & Blei, A. (2016). **Atlas of Urban Expansion** (Vol. 1: area and Density). Accra: New York: New York University, Nairobi : UN-Habitat, and Cambridge, MA : Lincoln Institute of Land Policy, 2016.

[13] Angel, S., Cievco, D. & Blei, A. (2011). **Making room for a planet of cities.** Cambridge : Lincoln Institute of Policy.

[14] Lelo Nzuzi, F. (2011). **Kinshasa : Planification et Aménagement.** Paris: L'Harmattan

[15] Jean-Pierre C. (2005). Occupation du sol. Maison de la télédétection

[16] Alexis C., Peter F. and Richard W. (2005), « What is land cover? », Environment and Planning B: Planning and Design, n° 32, 2005, p. 199–209. DOI: 10.1068/b31135

[17]M. Jia, Z. Wang, D. Mao, C. Ren, K. Song, C. Zhao, C. Wang, X. Xiao, Y. Wang, (2023). Mapping Global Distribution of Mangrove Forests at 10-m Resolution, Science Bulletin. https://doi.org/10.1016/j.scib.2023.05.004

[18] C. Zhao, M. Jia, Z. Wang, D. Mao, Y. Wang (2023). Toward a better understanding of coastal salt marsh mapping: a case from China using dual-temporal images, Rem. Sens. Environ. 295, 113664. **DOI**: 10.1016/j.rse.2023.113664

[19] E.E. Maeda, J. Heiskanen, L.E. Arag˜ ao, J. Rinne (2014). Can MODIS EVI monitor ecosystem productivity in the Amazon rainforest? Geophys. Res. Lett. 41 (20) 7176–7183. **DOI**: 10.1002/2014GL061535

[20] Bhatia, P.L. Teo, M. Li, J.Y.B. Lee, M.X.J. Chan, T.W. Yeo, M. Mathur, S. Tagore, Yeo, S.H. George, S. Arulkumaran (2021). Dinoprostone vaginal insert (DVI) versus adjunctive sweeping of membranes and DVI for term induction of labor, J. Obstet. Gynaecol. Res. 47 (9) 3171–3178. **DOI**: 10.1111/jog.14907

[21] Franch, E.F. Vermote, S. Skakun, J.C. Roger, I. Becker-Reshef, E. Murphy, C. Justice (2019). Remote sensing based yield monitoring: application to winter wheat in United States and Ukraine, Int. J. Appl. Earth Obs. Geoinf. 76 112–127. **DOI**: 10.1016/j.jag.2018.11.012

[22] S. Manna, B. Raychaudhuri (2020). Mapping distribution of Sundarban mangroves using Sentinel-2 data and new spectral metric for detecting their health condition, Geocarto Int. 35 (4) 434–452. **DOI**: 10.1080/10106049.2018.1520923

[23] L. Chai, H. Jiang, W.T. Crow, S. Liu, S. Zhao, J. Liu, S. Yang(2020). Estimating corn canopy water content from normalized difference water index (NDWI): an optimized NDWI-Based scheme and its feasibility for retrieving corn VWC, IEEE Trans. Geosci. Rem. Sens. 59 (10) 8168–8181. DOI: 10.1109/TGRS.2020.3041039

[24] K. Li, Y. Chen (2018). A Genetic Algorithm-based urban cluster automatic threshold method by combining VIIRS DNB, NDVI, and NDBI to monitor urbanization, Rem. Sens. 10 (2) 277. **DOI**: 10.3390/rs10020277

[25] Nagy, A. Szabo, ´ O.D. Adeniyi, J. Tam´ as (2021). Wheat yield forecasting for the Tisza River catchment using landsat 8 NDVI and SAVI time series and reported crop statistics, Agronomy 11 (4) 652.

[26] Y. Zhang, X. Ban, E. Li, Z. Wang, F. Xiao, Evaluating ecological health in the middle-lower reaches of the Hanjiang River with cascade reservoirs using the Planktonic index of biotic integrity (P-IBI), Ecol. Indicat. 114 (2020), 106282. **DOI**: 10.1016/j.ecolind.2020.106282

[27] T. Hou, W. Sun, C. Chen, G. Yang, X. Meng, J. Peng (2022). Marine floating raft aquaculture extraction of hyperspectral remote sensing images based decision tree algorithm, Int. J. Appl. Earth Obs. Geoinf. 111, 102846. **DOI**: 10.1016/j.jag.2022.102846

[28] Alem, S. Kumar (2022). Deep learning models performance evaluations for remote sensed image classification, IEEE Access 10 111784–111793. **DOI:** 10.1109/ACCESS.2022.3215264

[29] Damien S. M. and Mark A. F. (2018). User Guide to Collection 6 MODIS Land Cover (MCD12Q1 and MCD12C1) Product.

[30] Danny Holten (2006). Hierarchical Edge Bundles: Visualization of Adjacency Relations in Hierarchical Data. 1077-2626/06/$20.00 © 2006 IEEE. Available at: https://aviz.fr/wiki/uploads/Teaching2014/bundles_infovis.pdf

***Corresponding author:** *innocent.mufungizi@unikin.ac.cd*

DOI: 10.31695/IJASRE.2023.9.11.6